Comparative Study of the Large Eddy Simulations with the Lattice Boltzmann Method Using the Wall-Adapting Local Eddy-Viscosity and Vreman Subgrid Scale Models

CHIN. PHYS. LETT. Vol. 29, No. 10 (2012) 104706

Comparative Study of the Large Eddy Simulations with the Lattice Boltzmann Method Using the Wall-Adapting Local Eddy-Viscosity and Vreman Subgrid Scale Models *

LIU Ming(刘明)[1], CHEN Xiao-Peng(陈效鹏)[1**], Kannan N. Premnath[2]

[1]*School of Mechanics, Civil Engineering and Architecture, Northwestern Polytechnical University, Xi'an 710072*
[2]*Department of Mechanical Engineering, University of Colorado Denver, Denver 80217-3364, USA*

(Received 24 April 2012)

The wall-adapting local eddy-viscosity (WALE) and Vreman subgrid scale models for large eddy simulations are compared within the framework of a generalised lattice Boltzmann method. Fully developed turbulent flows near a flat wall are simulated with the two models for the shear (or friction) Reynolds number of 183.6. Compared to the direct numerical simulation (DNS), damped eddy viscosity in the vicinity of the wall and a correct velocity profile in the transitional region are achieved by both the models without dynamic procedures. The turbulent statistics, including, e.g., root-mean-square velocity fluctuations, also agree well with the DNS results. The comparison also shows that the WALE model predicts excellent damped eddy viscosity near the wall.

PACS: 47.11.Qr, 47.27.N−, 02.60.−x DOI: 10.1088/0256-307X/29/10/104706

The lattice Boltzmann method (LBM) has received considerable interest in the past few decades as an efficient method of computing a variety of fluid flows, ranging from low-Reynolds-number flows to highly turbulent flows.[1] It is one of the mesoscopic methods rooting in particle dynamics. Basically, the particles are supposed to collide and stream during the evolution on grid nodes of a lattice. Through multiscale expansion[2] or asymptotic analysis,[3] the moments of the distribution functions can be demonstrated to solve the Navier–Stokes and continuity equations. The scheme is conservative and the higher moments contain local gradient information of the lower moments, which could also be used to compute the strain rate for large eddy simulation (LES) models as demonstrated by several authors.[4,5] Early lattice Boltzmann models, e.g. the single relaxation time (SRT) model, suffer great difficulties for large Reynolds number flows due to the numerical instability.[1] In 1992, d'Humieres proposed a multiple-relaxation-time (MRT) LB model, where the moments of the density populations are relaxed independently.[6] It improves the feasibility of the LBM on a large Reynolds number flow by suppressing the short-length pressure wave with an adjustable bulk viscosity.[7–9] On the other hand, by introducing turbulent viscosity, the stability of the method could be improved.

Pioneering work was carried out by Hou *et al.*[4] applying the Smagorinsky subgrid scale (SGS) LES turbulent model in 2D SRT LBM. Krafczyk and Tölke[5] further incorporated 3D MRT LBM with the SGS model and demonstrated its feasibility. However, the Smagorinsky model fails to accurately predict the flow close to solid walls and the transitional region, due to its excessive eddy viscosity and isotropy assumption. For a long time, many accurate modified LES models have been explored by researchers.[10,11] In particular, in some earlier studies, semi-empirical damping functions,[12] dynamic procedures,[13] and shear-improved dissipative modeling[14] were considered in the LBM resulting in a better representation of near-wall turbulence behaviour. Recently, Nicoud and Vreman published their models, named as the wall-adapting local eddy-viscosity (WALE)[15] and Vreman models,[16] respectively. Both strain-rate and vorticity were considered to calculate eddy viscosity in the former model, which has been applied in LBM simulations.[17] While in the latter one, the second principal invariant of the velocity gradient was applied. Both of the models are straight forward to implement without applying a damping function or dynamic procedures, but accurately predict the flow in the near-wall and transitional regions.[15,16] In this Letter, a turbulent flow in a bounded domain is simulated with the LBM coupled WALE and Vreman SGS models, and a comparison of the two turbulent models is conducted. A shear Reynolds number of 183.6 is adopted in the numerical simulation. The turbulent statistics using the two models are analyzed and compared.

The forced generalised LBE (GLBE) reads[8,18]

$$\begin{aligned} & f_\alpha(\boldsymbol{x}+\boldsymbol{e}_\alpha\delta_t, t+\delta_t) - f_\alpha(\boldsymbol{x}, t) \\ = & -\sum_\beta \Lambda_{\alpha\beta}(f_\beta - f_\beta^{\mathrm{eq}}) \\ & +\sum_\beta (I_{\alpha\beta} - \frac{1}{2}\Lambda_{\alpha\beta}) S_\beta \delta_t, \end{aligned} \tag{1}$$

where $\boldsymbol{x}$ denotes the grid location, $\boldsymbol{e}_\alpha$ the discretized microscopic velocity, t and δ_t the time and time step, f_α the density distribution functions in direction α

*Supported by the Research Fund for the Doctoral Program of Higher Education of China, the National Natural Science Foundation of China under Grant Nos 10902087 and 11172241, and the National Hi-Tech Research and Development Program of China under Grant No 2012AA011803.

**Corresponding author. Email: xchen76@nwpu.edu.cn

(subscripts α and β run in the range 0–18 for the 3D D3Q19 model), respectively. On the right-hand side (RHS) of the equation, the first term represents the collision operation, with $\Lambda_{\alpha\beta}$ being the collision matrix. Here, we adopt a low-Mach-number truncated Maxwell distribution as the equilibrium function for each distribution,

$$f_\beta^{\rm eq} = f_\beta^{\rm Maxwell}(\rho, \boldsymbol{u}) = \omega_\alpha\Big\{1 + \frac{\boldsymbol{e}_\alpha \cdot \boldsymbol{u}}{c_s^2} + \frac{(\boldsymbol{e}_\alpha \cdot \boldsymbol{u})^2}{2c_s^4} - \frac{1}{2}\frac{\boldsymbol{u}\cdot\boldsymbol{u}}{c_s^2}\Big\},$$

$$\omega_\alpha = \begin{cases} \frac{1}{3}, & \alpha = 0, \\ \frac{1}{18}, & \alpha = 1, \ldots, 6, \\ \frac{1}{36}, & \alpha = 7, \ldots, 18, \end{cases}$$

where c_s denotes the sound speed.

The collision term can be further transformed from the population space to the moment space, $|m\rangle = M \cdot |f\rangle$.[6] One of the moment spaces could be chosen as

$$|m\rangle = (\rho, e, e^2,\ j_x,\ q_x,\ j_y,\ q_y,\ j_z,\ q_z,\ 3p_{xx},\ 3\pi_{xx}, p_{ww},\ \pi_{ww},\ p_{xy},\ p_{yz},\ p_{zx}, m_x, m_y, m_z)^T.$$

Among these nineteen moments, the density ρ and the momentum $\boldsymbol{j} = (j_x, j_y, j_z)$ are conserved moments for the athermal LBE model; e, e^2 and q are energy, energy square and heat flux, respectively; p_{xx}, p_{xy}, p_{xz} and p_{yz} denote the symmetric traceless shear stress tensor components. The other two normal components of the viscous stress tensor, p_{yy} and p_{zz}, can be constructed from p_{xx} and p_{ww}, where $p_{ww} = p_{yy} - p_{zz}$. For the left five values, the first two have the same symmetry as the diagonal part of the traceless viscous tensor p_{ij}, while the last three vectors are parts of a third rank tensor, with the symmetry of $j_k p_{mn}$. In the equation, the collision matrix can be transformed to

$$\hat{S} = M \cdot \Lambda \cdot M^{-1} = \mathrm{diag}(s_0,\ s_1,\ s_2,\ s_3,\ s_4,\ s_5,\ s_6,\ s_7,\ s_8,\ s_9, s_{10},\ s_{11},\ s_{12},\ s_{13},\ s_{14},\ s_{15},\ s_{16},\ s_{17},\ s_{18}).$$

For the D3Q19 model, shear and bulk viscosity read, respectively,

$$\zeta = \frac{2}{9}\Big(\frac{1}{s_1} - \frac{1}{2}\Big)\delta t,$$
$$\nu = \frac{1}{3}\Big(\frac{1}{s_\beta} - \frac{1}{2}\Big)\delta t,\ \beta = 9, 11, 13, 14, 15. \quad (2)$$

Back to Eq. (1) again, the last term on the RHS represents the influences of the external forces $\boldsymbol{F}$,

$$S_\alpha = \frac{(e_{\alpha j} - u_j)F_j}{\rho c_s^2} f_\alpha^{\rm Maxwell}(\rho, \boldsymbol{u}),$$

as in Refs. [18,19]. Neglecting terms of order $O(Ma^2)$, we can achieve

$$S_\alpha = \omega_\alpha[\frac{3}{c^2}(e_{\alpha i} - u_i) + \frac{9}{c^4}(\boldsymbol{e}_\alpha \cdot \boldsymbol{u})e_{\alpha i}]F_i.$$

To include turbulence effects into the filtered LBE[4] (or the NS equations), the SGS stress, representing the effects of the unresolved scales on the resolved scales, is modeled as

$$\tau_{\alpha\beta} - \frac{\delta_{\alpha\beta}}{3}\tau_{\kappa\kappa} = -2\nu_t \bar{S}_{\alpha\beta} = -2C_X^2 \Delta^2 \overline{OP}\bar{S}_{\alpha\beta}, \quad (3)$$

where C_X denotes a constant of the model, Δ the subgrid characteristic length scale (in practice, the size of the mesh) and $\overline{OP}$ is an operator of space and time and is defined from the resolved fields. In LBM, the total viscosity reads

$$\nu_{\rm total} = \nu_0 + \nu_t. \quad (4)$$

In the WALE model,[15] $\overline{OP}$ is calculated from the symmetric part of the resolved velocity gradient,

$$\bar{S}_{\alpha\beta} = \frac{1}{2}\Big(\frac{\partial \bar{u}_\alpha}{\partial x_\beta} + \frac{\partial \bar{u}_\beta}{\partial x_\alpha}\Big),$$

and the anti-symmetric part,

$$\bar{\Omega}_{\alpha\beta} = \frac{1}{2}\Big(\frac{\partial \bar{u}_\alpha}{\partial x_\beta} - \frac{\partial \bar{u}_\beta}{\partial x_\alpha}\Big),$$

as

$$\overline{OP} = \frac{(g_{\alpha\beta}g_{\alpha\beta})^{3/2}}{(\bar{S}_{\alpha\beta}\bar{S}_{\alpha\beta})^{5/2} + (g_{\alpha\beta}g_{\alpha\beta})^{5/4}},$$
$$g_{\alpha\beta} = \bar{S}_{\alpha\gamma}\bar{S}_{\gamma\beta} + \bar{\Omega}_{\alpha\gamma}\bar{\Omega}_{\gamma\beta} - \frac{1}{3}\delta_{\alpha\beta}(S^2 - \Omega^2), \quad (5)$$

$C_X = 0.5$ and $S^2 = \bar{S}_{\alpha\beta}\bar{S}_{\alpha\beta}$, $\Omega^2 = \bar{\Omega}_{\alpha\beta}\bar{\Omega}_{\alpha\beta}$. We note that $\overline{OP}$ behaves as z^3 near a wall,[15] where z is the distance from the wall. In this model, both $\bar{S}_{\alpha\beta}$ and $\bar{\Omega}_{\alpha\beta}$ are calculated by a finite difference method. On the other hand, a more accurate calculation of the strain rate tensor can also be obtained from the second order moments and the scheme has a second order precision.[4,5]

Vreman[16] chose another template to calculate the $\overline{OP}$,

$$\overline{OP} = \sqrt{\frac{B_\beta}{\alpha_{ij}\alpha_{ij}}}, \quad (6)$$

where α_{ij} is the resolved velocity gradient, and $B_\beta = \beta_{11}\beta_{22} - \beta_{12}^2 + \beta_{11}\beta_{33} - \beta_{13}^2 + \beta_{22}\beta_{33} - \beta_{23}^2$, $\beta_{ij} = \alpha_{mi}\alpha_{mj}$. The model constant C_X is related to the Smagorinsky constant C_S by $C_X \approx \sqrt{2.5}C_S$.

Like the Smagorinsky SGS model, both the models are easy to compute in actual LES, since they only need one local filter stencil and the first-order derivatives of the velocity field.

In order to compare the accuracy of the two SGS models for LES using GLBE, we have considered a prototypical problem involving turbulent open channel flow, for which detailed DNS and experimental data are available. Following Ref. [12], Fig. 1 shows the schematic diagram of the computational domain.

A 3D fully developed turbulent channel flow was simulated. The dimensionless parameter, i.e. the shear Reynolds number, $Re_* = u_* H/\nu_0 = 183.6$, where H denotes half the height of the channel and u_* the characteristic shear velocity on the wall. Slip and non-slip boundary conditions are imposed on the top and bottom boundaries, respectively, and periodic boundary conditions on left/right and front/backward sides. The width and length of the channel are $3H$ and $6H$, respectively (in the testing cases, $H = 45\Delta$). In this domain, it is large enough for a sufficient number of wall-layer streaks.[20] The grid resolution is chosen as $\Delta^+ = \Delta/\delta_\nu = 4.08$, where $\delta_\nu = \nu_0/u_*$ represents the characteristic length. Using the half-way bounce-back boundary condition scheme,[1,12] the distance of the first layer of grid nodes are $\Delta^+_{nw} = \Delta^+/2 = 2.04$. It is important that the resolved scale should be able to resolve the local dissipative or Kolmogorov length scale $\eta = (\nu_0^3/\varepsilon)^{1/4}$, i.e., $\Delta^+_{nw} \leq O(\eta^+)$.[21] Generally, $1.5\eta^+$–$2.0\eta^+$ is the upper limit of grid-spacing, above this, the small turbulence motion of the bounded flow will not be resolved well. As we know, $\eta^+ = 1.5$–2.0 at the wall and it increases with the increasing distance from the wall.[22] Thus the grid scale we choose is expected to resolve the small turbulent structures.

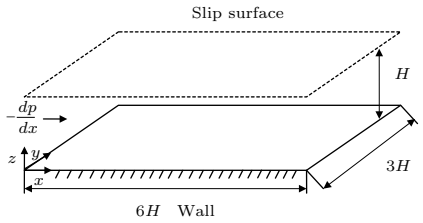

Fig. 1. Schematic diagram of computational domain.

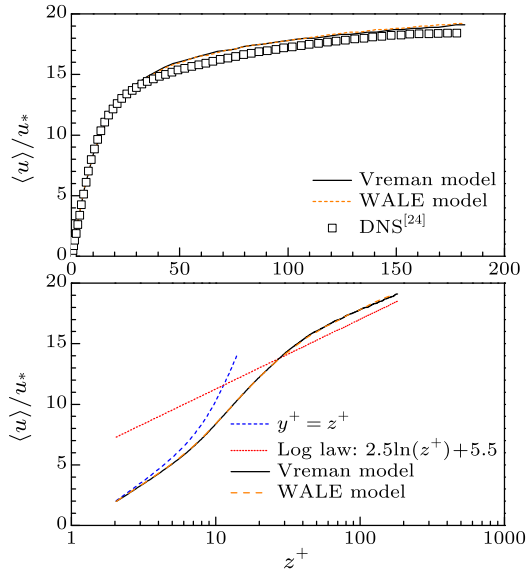

Fig. 2. (a) Mean streamwise velocity profile for fully developed wall-bounded channel flow ($Re_* = 183.6$), (b) comparison of mean velocity profile with a logarithm law inside the boundary layer.

The initial mean velocity is specified to satisfy the $1/7^{\text{th}}$ power law,[22] with divergence free perturbations.[20] Then, the corresponding density populations or moments calculated with a specific initial procedure[23] to initialise the pressure and non-equilibrium parts of the distribution functions. Using $\boldsymbol{F} = -\hat{x}dp/dx = \hat{x}\tau_w/H = \hat{x}\rho u_*^2/H$ as the external driving force, the GLBE computations are carried out until stationary turbulence statistics are obtained, as measured by the invariant Reynolds stresses profiles. The peak Mach number of the mean flow is about 0.28. This initial run was carried out for a duration of $50T^*$ ($T^* = \frac{H}{u^*}$, the characteristic time scale). The averaging of various flow quantities is carried out in time as well as in space in the homogeneous directions, i.e., over the horizontal planes, by an additional run for a period of $16T^*$.

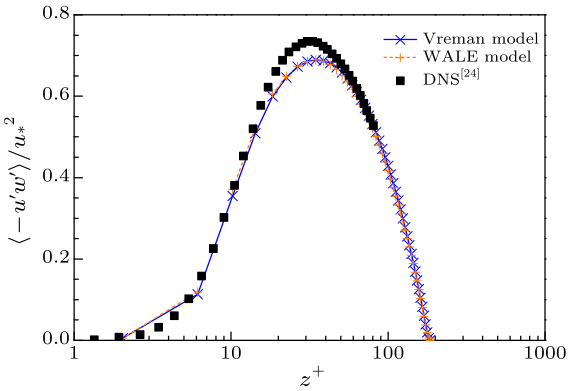

Fig. 3. Reynold stress profile for fully developed turbulent channel flow.

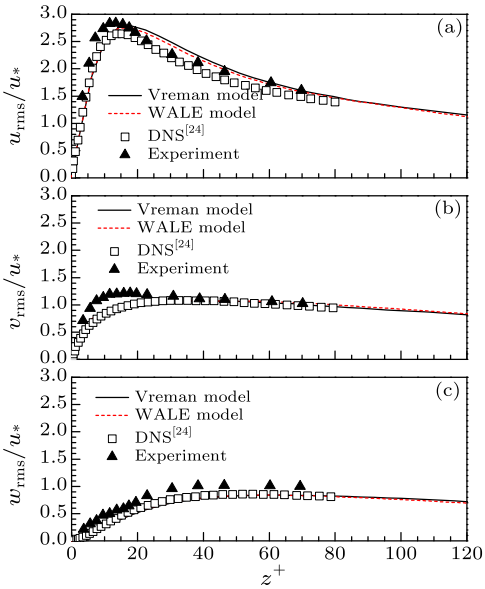

Fig. 4. (a) The rms streamwise velocity fluctuations for fully developed turbulent channel flow; (b) the rms spanwise velocity fluctuations for a fully developed turbulent channel flow; (c) the rms wall-normal velocity fluctuations for a fully developed turbulent channel flow; at $Re_* = 183.6$.

The mean velocity profile, normalised by the wall

shear velocity u^*, as a function of the normalised distance from the wall, i.e. $z^+ = z/\delta_\nu$, is shown in Fig. 2(a) and the DNS data by Kim *et al.*[24] are plotted as well. The GLBM results are valid for the so-called logarithm law. It can be further shown in Fig. 2(b), where, for $z^+ > 30$, the mean velocity satisfies the logarithm law, i.e., $u^+ = A \ln z^+ + B^+$, and the coefficients depend on the flow parameters and roughness of the wall. For $Re_* \sim 180$, $A = 2.5$ and $B = 5.5$ are known to be reasonable for smooth walls.[20,22] The computed mean velocity profiles coincide with each other with less than 0.5% discrepancy, and follow the DNS data fairly closely with about 5% difference. We believe this error to be due to the coarse grid, slightly high Ma number and the numerical dissipation of the computational approach for LES.

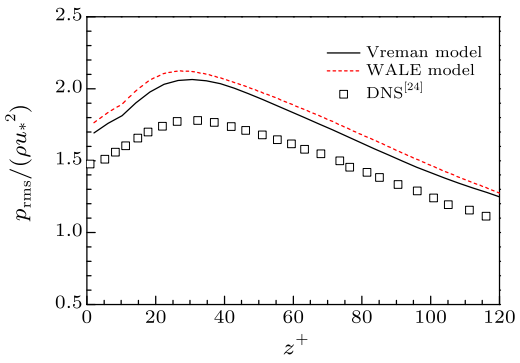

Fig. 5. The rms pressure fluctuations for a fully developed turbulent channel flow at $Re_* = 183.6$.

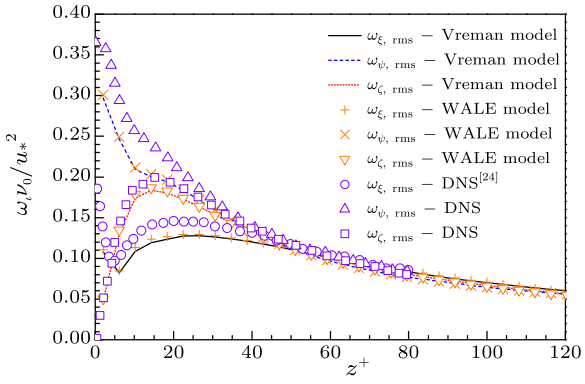

Fig. 6. The rms vorticity fluctuations for a fully developed turbulent channel flow at $Re_* = 183.6$.

Figure 3 shows the Reynolds stress, normalised by the wall shear stress, obtained by the WALE and Vreman SGS models. Again, the two results are quite close. A comparison with DNS[24] shows the LBM's good accuracies, except around $z^+ \sim 20$, where the error is about 7%, which is probably due to the relatively low grid resolution and Ma number effects.

Figures 4(a)–4(c) show the span/stream-wise and wall-normal rms velocity fluctuations, which are normalised by characteristic wall-shear velocity (u^*). It is shown that the discrepancy between the WALE and Vreman models is less than 3%. Compared to the DNS results, errors about 10% are found. However, the LBM results are closer to Kreplin's experimental data.[25]

Further comparisons are carried out for rms pressure fluctuation and vorticity components fluctuations, as in Figs. 5 and 6. The aforementioned findings are validated. In general, both WALE and Vreman SGS predicted variables are qualitatively comparable to the DNS results and the two SGS models give very similar results. As described in Ref. [12] and the references therein, the compressibility and filter effects might be the reasons for the deviations in Figs. 5 and 6, respectively, as compared to the DNS results.

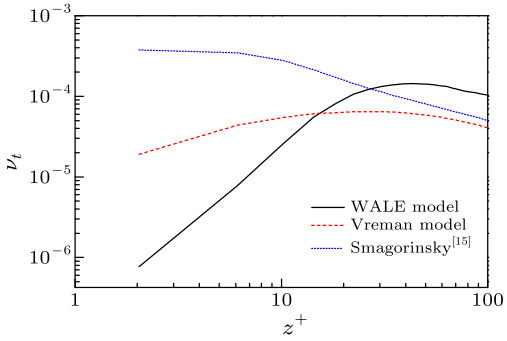

Fig. 7. Eddy viscosity in the near wall region comparison at $Re_* = 183.6$.

Table 1. Computation time for the WALE and Vreman SGS models (1000 iterations), compiled with different optimisation parameters (t_0: computation time without using the optimisation parameters, $t_{o,1}$, $t_{o,2}$, $t_{o,3}$: computation time with using the different optimisation parameters.

SGS model	t_0 (s)	$t_{o,1}$ (s)	$t_{o,2}$ (s)	$t_{o,3}$ (s)
Vreman	3859.19	1919.66	1968.42	2187.59
WALE	5133.04	3263.30	3273.98	3464.52

The comparison of eddy viscosity in the near wall region shows (Fig. 7) that both the WALE and Vreman's models predict the damped turbulent strength. However, the WALE model gives almost an ideal relation of $\nu_t \sim O(y^3)$. The results are unsurprising since it is one of the pre-restrictions in the WALE model.

In order to compare the computational costs for both the models, we ran the codes on TYAN S2932 (CPU: AMD 8378) with the RedHat 4.1.2 operating system using the GCC-4.1.2 compiler. We estimated the running time for 1000 iterations after the initialisation procedure, which are listed in Table 1 with different compiler optimisation parameters. It is shown that the Vreman model saves about 40% computational time when compared to the WALE model.

In summary, the WALE and Vreman SGS models are compared to each other by simulating a fully developed turbulent flow in a channel, in the framework of a forced GLBM. Statistics, including averaged velocities, Reynolds stress, span/stream-wise/wall-normal rms velocity fluctuations (among others), are analyzed. The obtained results are very similar, showing a maximum discrepancy of ∼1% and both match with the DNS predictions quite well. The averaged stream-

wise velocity profile satisfies the logarithmic law in the transitional region of the boundary layer. Good accuracies are also achieved for the second order statistics, e.g. Reynolds stress and velocity fluctuations where errors are below 7%. The results also show that the WALE model predicts a reasonably damped eddy viscosity near the wall. Accordingly, the GLBE, coupled with a WALE or Vreman SGS model, appears to be a reliable approach for LES of wall-bounded turbulent flows. No dynamic procedures are applied and their implementation is straightforward. With respect to the computational cost, the Vreman model saves about 40% in comparison to the WALE model. Both the Vreman and WALE models can be further improved by eliminating the need to specify the single unknown constant that could depend on the flow being considered. As such, there have been some recent efforts to eliminate this remaining empiricism using a simple procedure and thus potentially allow an extension to complex flows and geometries,[26,27] which could be adopted for the LBM in future studies.

References

[1] Chen S Y and Doolen G D 1998 *Annu. Rev. Fluid Mech.* **30** 329
[2] Frisch U, d'Hummieres D, Hasslacher B, Lallemand P, Pomeau Y and Rivet J P 1987 *Complex Syst.* **1** 649
[3] Junk M, Klar A and Luo L S 2005 *J. Comput. Phys.* **210** 676
[4] Hou S, Sterling J D, Chen S and Doolen G D 1996 *Fields Inst. Commun.* **6** 151
[5] Krafczyk M, Tölke J and Luo L S 2003 *Int. J. Mod. Phys.* B **17** 33
[6] d'Humieres D 1992 *Prog. Astron. Aero.* **159** 450
[7] Lallemand P and Luo L S 2000 *Phys. Rev.* E **61** 6546
[8] d'Humieres D 2002 *Philos. Trans. R. Soc.* A **360** 437
[9] Chai Z H, Shi B C and Zheng L 2006 *Chin. Phys.* **15** 1855
[10] Germano M, Piomelli U, Moin P and Cabot W H 1991 *Phys. Fluids* **3** 1761
[11] Lilly D K 1992 *Phys. Fluids* **4** 633
[12] Premnath K N, Pattison M J and Banerjee S 2009 *Phys. Rev.* E **79** 026703
[13] Premnath K N, PattisonM J and Banerjee S 2009 *Physica* A **388** 2640
[14] Jafari S and Rahnama M 2011 *Int. J. Numer. Methods Fluids* **67** 700
[15] Nicoud F and Ducros F 1999 *Flow. Turb. Combust.* **62** 183
[16] Vreman A W 2004 *Phys. Fluids* **16** 3670
[17] Weickert M, Teike G, Schmidt O and Sommerfeld M 2010 *Comput. Math. Appl.* **59** 2200
[18] Premnath K N and Abraham J 2007 *J. Comput. Phys.* **224** 539
[19] He X, Shan X and Doolen G D 1998 *Phys. Rev.* E **57** R13
[20] Lam K 1989 *PhD Thesis* (University of California, Santa Barbara, CA)
[21] Moin P and Mahesh K 1998 *Annu. Rev. Fluid Mech.* **30** 539
[22] Pop S 2000 *Turb. Flow* (New York: Cambridge University Press)
[23] Mei R, Luo L S, Lallemand P and d'Humieres D 2006 *Comput. Fluids* **35** 855
[24] Kim J, Moin P and Moser R J 1987 *J. Fluid Mech.* **177** 133
[25] Kreplin H and Eckelmann H 1979 *Phys. Fluids* **22** 1233
[26] You D and Moin P 2007 *Phys. Fluids* **19** 065110
[27] Nicoud F, Toda H B, Cabrit O, Bose S and Lee J 2011 *Phys. Fluids* **23** 085106